THE ASTROPHYSICAL JOURNAL, 554:L55–L58, 2001 June 10
© 2001. The American Astronomical Society. All rights reserved. Printed in U.S.A.

CHANDRA DETECTION OF DOPPLER-SHIFTED X-RAY LINE PROFILES FROM THE WIND OF ζ PUPPIS (O4 f)

J. P. CASSINELLI,[1] N. A. MILLER,[1] W. L. WALDRON,[2] J. J. MACFARLANE,[3] AND D. H. COHEN[3,4]

Received 2001 February 16; accepted 2001 May 7; published 2001 May 31

ABSTRACT

We report on a 67 ks High-Energy Transmission Grating observation of the optically brightest early O star ζ Puppis (O4 f). Many resolved X-ray lines are seen in the spectra over a wavelength range of 5–25 Å. *Chandra* has sufficient spectral resolution to study the velocity structure of isolated X-ray line profiles and to distinguish the individual forbidden, intercombination, and resonance (*fir*) emission lines in several He-like ions, even where the individual components are strongly Doppler-broadened. In contrast to X-ray line profiles in other hot stars, ζ Pup shows blueshifted and skewed line profiles, providing the clearest and most direct evidence that the X-ray sources are embedded in the stellar wind. The broader the line, the greater the blueward centroid shift tends to be. The N VII line at 24.78 Å is a special case, showing a flat-topped profile. This indicates that it is formed in regions beyond most of the wind attenuation. The sensitivity of the He-like ion *fir* lines to a strong UV radiation field is used to derive the radial distances at which lines of S XV, Si XIII, Mg XI, Ne IX, and O VII originate. The formation radii correspond well with a continuum optical depth of unity at the wavelength of each line complex, indicating that the X-ray line emission is distributed throughout the stellar wind. However, the S XV emission lines form deeper in the wind than expected from standard wind-shock models.

Subject headings: line: profiles — stars: early-type — stars: individual (ζ Puppis) — stars: mass loss — stars: winds, outflows — X-rays: stars

1. INTRODUCTION

The O4 f star ζ Puppis has for decades been at the cutting edge of research regarding early-type stars because of its optical and UV brightness. In addition, because of the low interstellar attenuation, ζ Pup has been the prime X-ray target to study soft X-ray emission from O stars. Researchers have looked to this source to settle outstanding controversies about the physical location, quantity, and nature of the hot X-ray–emitting plasma on OB stars. In this Letter, we present the highest resolution X-ray spectrum of ζ Pup ever measured and explore the physical mechanism of hot star X-ray production.

Prior to the discovery of X-ray emission from O stars (Harnden et al. 1979; Seward et al. 1979), Cassinelli & Olson (1979) postulated thin base coronal zones as a source for X-rays to explain the observed UV superionization (Lamers & Morton 1976) by way of the Auger effect. The coronal models (Cassinelli & Olson 1979; Waldron 1984) predicted an X-ray absorption at the oxygen K-shell edge larger than that observed with the *Einstein* solid state spectrometer (Cassinelli & Swank 1983) and the *Broad Band X-Ray Telescope* (Corcoran et al. 1993). These observations, as well as detailed modeling of the superionization profiles (MacFarlane et al. 1993) and lack of detection of the iron "green line" (Baade & Lucy 1987) in ζ Pup, caused the coronal model to fall out of favor. Increasingly, a consensus formed around a wind-shock picture in which a series of shocks, perhaps related to the line-force instability (Lucy 1982; Owocki, Castor, & Rybicki 1988), causes hot, X-ray–emitting gas to be distributed *throughout* the dense stellar wind of ζ Pup and other OB stars. Wind-shock models developed by Lucy & White (1980), Feldmeier et al. (1997a), and others consistently failed to predict the high levels of X-ray emission observed in the brightest O stars like ζ Pup, leading to the suggestion that perturbations somehow form and propagate up from the photosphere into the wind and drive stronger shocks (Feldmeier 1995; Feldmeier, Puls, & Pauldrach 1997b). Broadband X-ray observations of ζ Pup (Corcoran et al. 1993; Hillier et al. 1993) indicate that some wind attenuation is affecting the soft X-ray flux. However, with the advent of *Chandra* and *XMM*, we can apply, for the first time, diagnostic emission-line ratios and measure line profiles to determine the locations and Doppler velocities of X-ray sources in the stellar wind of ζ Pup.

2. OBSERVATIONS AND CONSTRAINTS FROM HELIUM-LIKE FORBIDDEN, INTERCOMBINATION, AND RESONANCE LINE RATIOS

We obtained a 67 ks *Chandra* High-Energy Transmission Grating Spectrometer (HETGS) observation of ζ Pup from 2000 March 28 (13^h31^m UT) to March 29 (09^h12^m UT). The standard pipeline tools were used to reprocess the data with the most recent calibration files available. Line emission is clearly evident in both the high-energy grating (HEG) and the medium-energy grating (MEG). The combined ± 1 order, background-subtracted, HETGS spectra are shown in Figure 1. Triads of He-like ions known as the forbidden, intercombination, and resonance (*fir*) lines (S XV, Si XIII, Mg XI, Ne IX, and O VII) are seen, in addition to isolated Lyα emission lines and numerous L-shell lines of iron, especially Fe XVII.

Traditionally, He-like ion f/i line ratios have been used to derive electron densities of X-ray line-emitting regions since the populations of the 2^3P levels are controlled by collisional excitations from the 2^3S level (Gabriel & Jordan 1969). However, when a strong external UV source is present, the excitation $2^3S \rightarrow 2^3P$ is predominantly radiative, and this means that the f/i ratio is no longer a density diagnostic, but rather it can be used to determine the strength of the UV radiation field (Blumenthal, Drake, & Tucker 1972). The UV wavelengths asso-

[1] Department of Astronomy, University of Wisconsin at Madison, 6521 Sterling Hall, 475 North Charter Street, Madison, WI 53706; cassinelli@astro.wisc.edu, nmiller@astro.wisc.edu.

[2] Emergent Information Technologies, Inc., 9314 Largo Drive West, Suite 250, Largo, MD 20774; wayne.waldron@emergent-it.com.

[3] Prism Computational Sciences, 16 North Carroll Street, Madison, WI 53703; jjm@prism-cs.com, cohen@prism-cs.com.

[4] Department of Physics and Astronomy, 500 College Avenue, Swarthmore College, Swarthmore, PA 19081; dcohen1@swarthmore.edu.

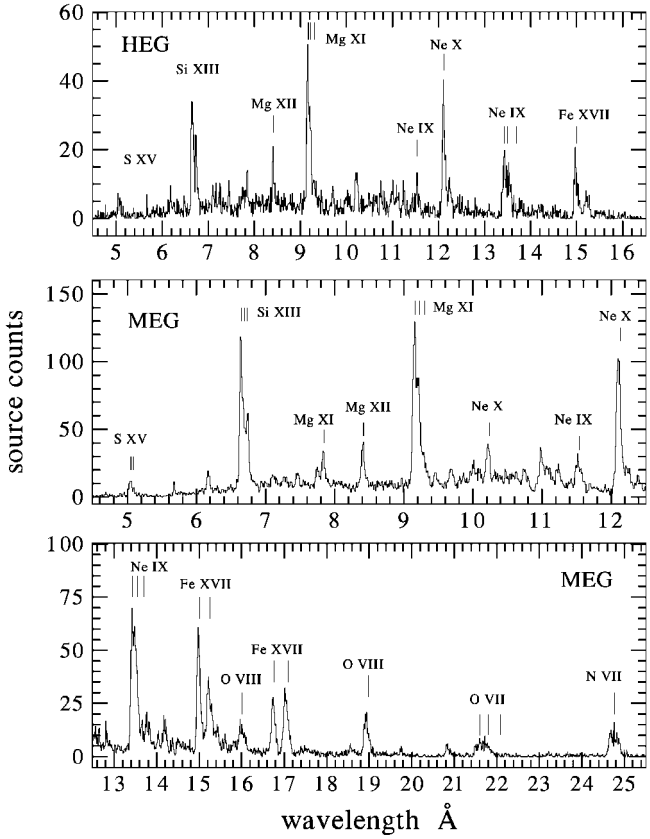


FIG. 1.—Co-added first-order, background-subtracted, *Chandra* HETGS HEG (*top panel*) and MEG (*bottom panels*) count spectra of ζ Pup. The ions responsible for the strongest line emissions are identified. The bin size is 0.01 Å.

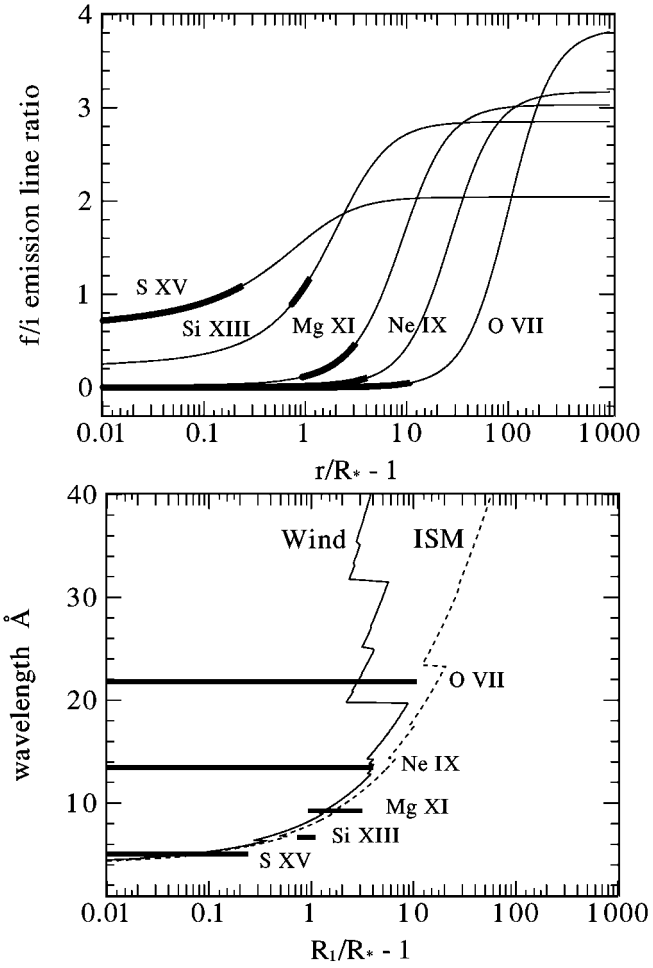


FIG. 2.—*Top panel*: Dependence of O VII, Ne IX, Mg XI, Si XIII, and S XV *f*/*i* ratios on radius due to the geometric dilution of the UV radiation field. The length of the thickened line for each ion extends over the range of the uncertainty in the *f*/*i* line ratio. *Bottom panel*: Radius of a wind continuum optical depth of unity as a function of wavelength. The thick horizontal lines correspond to the range in radii indicated in the top panel. For comparison, we also show the optical depth of unity radius assuming the neutral interstellar medium (ISM) opacity of Morrison & McCammon (1983).

ciated with the radiative excitation are in the range from ~650 to 1650 Å, where O-star UV fluxes are very strong. For ζ Pup's photospheric flux, we use a Kurucz (1993) model, assuming $T_{\rm eff} = 42{,}000$ K. Since the $2^3S \rightarrow 2^3P$ wavelengths are not on the Wien side of the spectrum, the model atmosphere fluxes are relatively well determined.

Waldron & Cassinelli (2001) demonstrated how the observed *f*/*i* line ratios can be used to derive the line formation radii from the geometric dilution of the photospheric radiation field in ζ Orionis (O9.5 Ia). Kahn et al. (2001) used a similar approach to derive line formation radii from their *XMM* Reflection Grating Spectrometer (RGS) spectrum of ζ Pup. Our *Chandra* HETG spectrum has better resolution at essentially all He-like ion wavelengths and greater sensitivity to the short-wavelength lines (e.g., Si and S) than the *XMM* spectrum. This high resolution is very important for O stars since their X-ray lines show strong broadening. The observed He-like *f*/*i* line ratios are listed in Table 1.

The top panel of Figure 2 shows the radii derived from our measurements of the He-like *f*/*i* ratios. The radii of line formation are seen to vary from ion to ion, with lines from high nuclear charge ions (Si and S) forming at small radii and from lower nuclear charge ion lines (O, Ne, and Mg) forming at larger radii. One might expect the *fir* line complexes for each element to be formed over a range of radii and not just in a thin shell. However, since the line emission is proportional to n_e^2, the observed emission in each line complex should be dominated by the densest regions (i.e., the smallest radius) from which the line radiation can escape. For ζ Ori, the *fir* formation location correlates with the associated radial optical depth of unity radius R_1. The optical depth is measured through the wind, using the continuum opacity at the wavelength of each triad of *fir* lines. Any line radiation that originates much below R_1 could not be seen by an external

TABLE 1
fir RATIO MEASUREMENTS

Ratio	S XV	Si XIII	Mg XI	Ne IX	O VII
f/*i*	0.61 ± 0.48	1.03 ± 0.14	0.29 ± 0.18	<0.1	<0.1
r/*i*	0.78 ± 0.54	2.00 ± 0.25	1.53 ± 0.13	1.44 ± 0.18	1.30 ± 0.6
$\mathcal{F}_{\rm tot}$[a]	0.81	3.06	3.26	5.77	3.56

[a] Total flux of the three lines in units of 10^{-13} ergs cm $^{-2}$ s $^{-1}$.

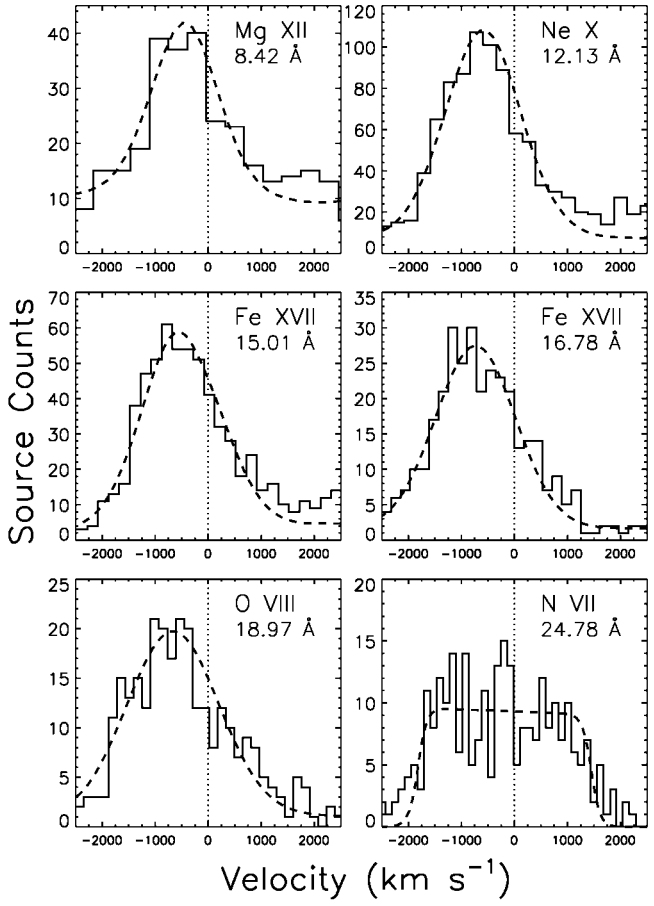


FIG. 3.—Six X-ray line profiles from the ζ Pup spectrum (*solid histograms*) with fits (*dashed curves*). The vertical dotted lines indicate the rest wavelengths for these transitions. The first five lines were fitted with Gaussians, while the N VII line was fitted with a box function because of its flat-topped shape. All functions shown have been convolved with the instrumental response. These functions are simultaneous fits to the MEG + 1 order and MEG − 1 order spectra but are shown here superposed on the co-added MEG first-order spectrum for the sake of brevity. The data have been binned to 0.01 Å. The fit parameters are given in Table 2.

observer. The wavelength dependence of R_1 for ζ Pup is shown in the bottom panel of Figure 2 using a β-law with $\beta = 0.75$ as the velocity law, the wind absorption cross sections in Waldron et al. (1998), and the stellar parameters of Lamers & Leitherer (1993; $R_* = 16\ R_\odot$, $\dot{M} = 2.4 \times 10^{-6}\ M_\odot\ \mathrm{yr}^{-1}$, and $v_\infty = 2200$ km s^{-1}).

An inspection of Figure 2 leads to the following conclusions: First, the He-like line formation radii are all consistent with their associated R_1-values, as expected from the above argument. Second, the f/i ratio of S XV indicates that hot plasma exists below $1.2R_*$ where the nominal wind velocity is less than 600 km s^{-1}. Most radiative instability simulations do not show strong shocks this close to the star (Feldmeier 1995; Owocki et al. 1988). However, using a velocity jump even half as large as the local wind velocity ($\Delta v = 300$ km s^{-1}) to calculate the shock temperature from $T = 1.4 \times 10^5$ K $(\Delta v/100$ km s$^{-1})^2$, we obtain a postshock temperature of 1 MK, which is too low to produce S XV. Thus, anomalously strong shock jumps are required deep in the wind. A similar conclusion was reached by Waldron & Cassinelli (2001), but for ζ Ori, the highest ion stage observed was Si XIII instead of the S XV seen here.

TABLE 2

LINE PROFILE WIDTHS AND CENTROID SHIFTS

Ion	$\lambda_{\rm rest}$ (Å)	$\mathcal{F}_{\rm line}$[a]	Source HWHM (km s^{-1})	Centroid Shift (km s^{-1})	R_1 (R_*)
Mg XII	8.42	0.30	610 ± 220	−440 ± 130	2.8
Ne X	12.13	3.33	780 ± 60	−570 ± 50	4.5
Fe XVII	15.01	4.74	800 ± 70	−500 ± 60	6.0
	16.78	2.24	850 ± 130	−730 ± 100	7.0
O VIII	18.97	3.05	990 ± 201	−670 ± 140	4.0
N VII	24.78	5.02	1570 ± 150	−120 ± 150	4.0

[a] Line flux in units of 10^{-13} ergs cm^{-2} s^{-1}.

3. EMISSION-LINE PROFILES

The most notable feature observed in our HETG spectrum of ζ Pup is the clear presence of blueshifted X-ray line centroids in all strong lines. This is in contrast to previous *Chandra* O-star observations (Schulz et al. 2000; Waldron & Cassinelli 2001) in which the lines were broad, symmetric, and unshifted. Although our line widths are comparable to other O-star observations, with a half-width at half-maximum (HWHM) of ~1000 km s^{-1}, our observation is the first *Chandra* detection of blueshifted and blueward-skewed X-ray line profiles in an O star. Figure 3 displays six ζ Pup X-ray lines arranged in order of wavelength. The results for the line fits are given in Table 2. There is an interesting progression that holds for these lines: the centroid shifts are generally larger for the broader lines, indicating a connection between radial location, wind absorption, and the Doppler broadening of the line emission. In Table 4 of their *XMM* study of ζ Pup, Kahn et al. (2001) list blueshifts of the Lyα lines of Ne X and O VIII. The blueshifts agree with ours to within 2 σ, and some of the discrepancy can be attributed to the absolute wavelength calibration uncertainties of the instruments (~100 km s^{-1} for the HETG (*Chandra* X-ray Center [CXC] 2000, p. 180; see den Herder et al. 2001 for the RGS). The *XMM* results show the same trend between shift and broadening. The N VII line is an exception to the trend in Table 2 because of its small centroid shift. It is different morphologically from the other lines (also noted by Kahn et al. 2001). It has a roughly flat-topped profile, so we use a box fit instead of a Gaussian to estimate the values for Table 2.

There is a blueward skewness observed in many of the ζ Pup lines that is not attributable to the HETGS line-response function (CXC 2000, p. 172). The blue sides of these lines tend to be steeper, while the red sides have a shallower slope. In general, the shape of these lines indicates wind broadening combined with attenuation as would arise from line formation in the marginally thick region near R_1. MacFarlane et al. (1991), Ignace (2001), and Owocki & Cohen (2001) demonstrate that emission-line profiles can provide important information about the spatial distribution of hot plasma within a stellar wind based both on the velocity dependence of the intrinsic emission and on the continuum attenuation across the line. Assuming isotropic emission, the redshifted emission from the back side of the wind is suppressed by the continuum opacity along the line of sight, while the blueshifted emission from the near side is less so. This leads to skewed, almost triangular-shaped lines in an optically thick wind.

In the ζ Ori HETG spectrum, Waldron & Cassinelli (2001) found that an optically thin model was needed to provide a reasonable fit because the lines were symmetric and unshifted. This fit required that the assumed mass-loss rate for ζ Ori be greatly reduced. For ζ Pup, we have the odd situation that the

blueward shift and asymmetric line profiles agree with what has long been expected for hot stars, but this is the first time that it has been so clearly observed in a *Chandra* spectrum for any star. We find that a fit can be made to the line profiles without making a significant reduction in the assumed mass-loss rate in contrast with the ζ Ori results.

The N VII line profile is different from those of the other ions, as can be seen in Figure 3 and Table 2. The Doppler half-width of this line is much greater than any of the other X-ray lines. This velocity of 1570 km s^{-1} can be compared with the terminal speed of 2200 km s^{-1} determined from UV wind lines. A flat-topped line profile such as this is expected from a fast-moving shell source suffering little or no wind attenuation (MacFarlane et al. 1991). Therefore, in contrast to the other observed lines, the N VII profile is probably formed well above its continuum optical depth of unity radius.

4. DISCUSSION AND SUMMARY

The *Chandra* HETG emission-line spectrum of ζ Pup, with its unprecedented resolution (in excess of $\lambda/\Delta\lambda = 1000$ for some lines) and sensitivity over a wide range of wavelengths, allows us to draw quantitative conclusions about the nature of the X-ray source on this prototypical hot star. Most importantly, we find that the wind plays an important, observable role in determining the X-ray line profiles of ζ Pup, in contrast to results for other stars.

We can begin to constrain the physical processes that lead to the production of the hot, X-ray–emitting plasma on this star. Taking all the He-like ions from oxygen through sulfur into account, the correlation between the formation radius of the *fir* lines and the radius at optical depth unity, R_1, we find evidence for a spatially distributed source of X-rays throughout the expanding wind.

There are two lines of particular interest in the development of future shock models: S XV and N VII. The shock jump required to produce S XV appears inconsistent with the expected local wind conditions, requiring a postshock flow velocity of approximately zero. Although this is not impossible for a shock model to reproduce, it places strong constraints on future modeling efforts. The N VII Lyα line may have a shape distinct from the other lines in our spectrum because it is formed in the outer regions of the wind where there is no further acceleration of the X-ray source region and little overlying wind attenuation. This *Chandra* HETG data set provides the most detailed and complete picture to date of an extended distribution of hot plasma embedded within a strong, optically thick stellar wind.

REFERENCES

Baade, D., & Lucy, L. B. 1987, A&A, 178, 213
Blumenthal, G. R., Drake, G. W. F., & Tucker, W. H. 1972, ApJ, 172, 205
Cassinelli, J. P., & Olson, G. L. 1979, ApJ, 229, 304
Cassinelli, J. P., & Swank, J. H. 1983, ApJ, 271, 681
Chandra X-Ray Center. 2000, *Chandra* Proposers' Observatory Guide, Version 3.0, TD 403.00.003 (Cambridge: CXC)
Corcoran, M. F., et al. 1993, ApJ, 412, 792
den Herder, J. W., et al. 2001, A&A, 365, L7
Feldmeier, A. 1995, A&A, 299, 523
Feldmeier, A., Kudritzki, R. P., Palsa, R., Pauldrach, A. W. A., & Puls, J. 1997, A&A, 320, 899
Feldmeier, A., Puls, J., & Pauldrach, A. W. A. 1997, A&A, 322, 878
Gabriel, A. H., & Jordan, C. 1969, MNRAS, 145, 241
Harnden, F. R., et al. 1979, ApJ, 234, L51
Hillier, D. J., Kudritzki, R. P., Pauldrach, A. W., Baade, D., Cassinelli, J. P., Puls, J., & Schmitt, J. H. M. M. 1993, A&A, 276, 117
Ignace, R. 2001, ApJ, 549, L119
Kahn, S. M., Leutenegger, M. A., Cottam, J., Rauw, G., Vreux, J.-M., den Boggende, A. J. F., Mewe, R., & Güdel, M. 2001, A&A, 365, L312
Kurucz, R. L. 1993, in IAU Colloq. 138, Peculiar versus Normal Phenomena in A-Type and Related Stars, ed. M. M. Dworetsky, F. Castelli, & R. Faraggiana (ASP Conf. Ser. 44; San Francisco: ASP), 87
Lamers, H. J. G. L. M., & Leitherer, C. 1993, ApJ, 412, 771
Lamers, H. J. G. L. M., & Morton, D. C. 1976, ApJS, 32, 715
Lucy, L. B. 1982, ApJ, 255, 286
Lucy, L. B., & White, R. L. 1980, ApJ, 241, 300
MacFarlane, J. J., Cassinelli, J. P., Welsh, B. Y., Vedder, P. W., Vallerga, J. V., & Waldron, W. L. 1991, ApJ, 380, 564
MacFarlane, J. J., Waldron, W. L., Corcoran, M. F., Wolff, M. J., Wang, P., & Cassinelli, J. P. 1993, ApJ, 419, 813
Morrison, R., & McCammon, D. 1983, ApJ, 270, 119
Owocki, S. P., Castor, J. I., & Rybicki, G. B. 1988, ApJ, 335, 914
Owocki, S. P., Cohen, D. H. 2001, ApJ, submitted (astro-ph/0101294)
Schulz, N. S., Canizares, C. R., Huenemoerder, D., & Lee, J. C. 2000, ApJ, 545, L135
Seward, F. D., Forman, W. R., Giacconi, R., Griffiths, R. E., Harnden, F. R., Jones, C., & Pye, J. P. 1979, ApJ, 234, L55
Waldron, W. L. 1984, ApJ, 282, 256
Waldron, W. L., Corcoran, M. F., Drake, S. A., & Smale, A. P. 1998, ApJS, 118, 217
Waldron, W. L., & Cassinelli, J. P. 2001, ApJ, 548, L45